Chinese Journal of
POLYMER SCIENCE

RESEARCH ARTICLE

https://doi.org/10.1007/s10118-022-2792-3
Chinese J. Polym. Sci. **2022**, *40*, 1422–1431

Dry-spun Polyimide Fibers with Excellent Thermal Stability, Intrinsic Flame Retardancy and Ultralow Smoke Release

Han Dong[a], Yu-Ping Wang[b], Xiu-Ting Li[a], Xin Zhao[a], Jie Dong[a*], and Qing-Hua Zhang[a*]

[a] *State Key Laboratory for Modification of Chemical Fibers and Polymer Materials, College of Materials Science and Engineering, Donghua University, Shanghai 201620, China*
[b] *Jiangsu New Vision Advanced Functional Fiber Innovation Center Co., Ltd., Suzhou 215000, China*

Electronic Supplementary Information

Abstract Polymer fiber with an ultrahigh thermal stability, superior flame retardancy and low smoke release during combustion is urgently needed and a crucial challenge for developing advanced fireproof textiles. In this study, a series of high-performance polyimide fibers are synthesized by copolymerizing 4,4'-diaminodiphenylmethane (MDA) into the pyromellitic dianhydride-*p*-phenylenediamine (PMDA-PDA) backbone for synergistically solving the technical challenge of poor fiber processing ability of these polyimides with a high inherent molecular rigidity. The glass transition temperature (T_g) of resultant fibers with the PDA molar ratio over 50 mol% reaches above 420 °C and their 10 wt% weight loss temperature ($T_{10\%}$) is within 543–633 °C. For the typical fiber containing 80 mol% of PDA, the limiting oxygen index (LOI) reaches 39% and exhibits a rapid self-extinguishing performance after deviating from the flame. Meanwhile, this fiber exhibits the minimum heat release rate of 14.1 kW/m^2 in a long ignition time of 813 s during combustion, revealing its better flame retardancy than the well-known Nomex fiber with a heat release rate of 140.6 kW/m^2 during the 120 s ignition. Meanwhile, the total smoke production of this polyimide fiber is only 1/9 of the Nomex fiber. Accordingly, the excellent flame retardancy of polyimide fibers indicating them more attractive as the fireproof materials in the field of emergency protection.

Keywords Polyimide fiber; Copolymerization; Thermal stability; Flame retardancy; Smoke release

Citation: Dong, H.; Wang, Y. P.; Li, X. T.; Zhao, X.; Dong, J.; Zhang, Q. H. Dry-spun polyimide fibers with excellent thermal stability, intrinsic flame retardancy and ultralow smoke release. *Chinese J. Polym. Sci.* **2022**, *40*, 1422–1431.

INTRODUCTION

Polymer fibers featured with a high axial ratio are the most useful materials for aerospace, industrial production and proliferating our everyday life, such as making composite materials for missile shells, manufacturing appealing clothing, making high temperature filter bag, preparing thermally protective fabrics for firefighters, soldiers, mine workers, *etc*. However, polymer fibers are organic in nature, making them susceptible to catch fire if they come into contact with a heating source or a flame.[1–5] In fact, during the past decades, the release of harmful gases in a fire has become the main cause of threats to people's health and safety.[6,7] During the burning of polymer fibers or fabrics, toxic volatiles (such as carbon monoxide) are released, which also posture a grave danger to the environment.[8] Therefore, improvement of flame retardancy and inhibiting the release of toxic gases of fibers in fire is highly vital and have aroused world-wide attention.

Generally, polymeric fibers have historically been made less flammable by incorporating small-molecule flame retardants (FR),[3,9–12] for example, the polyester fibers containing phosphorus-based FR by a chemical grafting or physical blending,[13] cotton fibers deposited with FR *via* a dip-coating,[14,15] sol-gel technique or layer-by-layer (LBL) assembly method,[16–18] and so on. However, the massive utilization of flame retardants always results in some unresolved issues, including the decreased processing ability and mechanical property, the environmental pollution due to release of flame retardants, the unresolved melt-drip characteristic of thermal plastic FR fibers, and so on. As an alternative method, physical blending of different fibers is also widely adopted to improve the flame retardant properties of materials, which always combines the advantages of individual fibers. Zhang *et al*. discovered that textiles comprised of flame retardant vinylon (FRV)/poly(*m*-phenylene isophthalamide) (PMIA) blended fibers showed a superior flame retardancy with a much higher time to ignition (TTI) and a lower peak heat release rate (HRR) than those of the neat components. [19] Wang *et al*. reduced the HRR from 249 W·g^{-1} for cotton to 22 W·g^{-1} for cotton/alginate by blending 80 wt% of alginate fiber, and meanwhile, the TTI increases 300% for the blended fiber.[20]

* Corresponding authors, E-mail: dj01@dhu.edu.cn (J.D.)
E-mail: qhzhang@dhu.edu.cn (Q.H.Z.)

Received March 6, 2022; Accepted May 30, 2022; Published online August 17, 2022

Additionally, physical blending also possesses some other advantages, including low-cost, easy processing, excellent mechanical performance and so forth. Unfortunately, an obvious limitation is that the flame retardancy of blended fibers is hardly to be accurately controlled according to the constituents due to the mutual interaction between components during combustion. For example, the polyester/cotton system showed a lower limiting oxygen index (LOI) and poorer flame retardancy than that of neat polyester or cotton due to the suppressed melts dropping of polyester and the intensive combustion of the blended fibers.[19,21] On the basis of above analysis, the target for new intrinsic flame retardant polymer fiber seems more attractive.

Fortunately, a handful of inherently flame-retardant polymeric fibers, *e.g.*, PMIA, poly(*p*-phenylene-terephthamide) (PPTA), polybenzimidazole (PBI), poly(*p*-phenylene-2,6-benzobisoxazole) (PBO) and polyimide (PI) fibers, *etc.*, have been developed and widely applied in various extreme conditions. Among of them, polyimide fibers are known to have some unique properties such as excellent chemical and radiation resistances, high thermal stability and char yield, good mechanical strength, in addition to intrinsic flame retardancy. Commercially available polyimide fibers, including P84 fibers from Evonik, Kermel fiber from Argos Soditic, Suplon fiber from Aoshen, *etc.*, have applications across many disciplines, including fireproof clothing for firefighters and soldiers, flame retardant insulation filler in spacecraft, *etc.*[22] It is noteworthy that the currently developed polyimide fibers are confronted with some common limits: (1) the thermal resistance of fibers is needed to be further improved to meet some severe requirements (*e.g.*, the T_g of P84 fiber is only ~320 °C);[23] (2) few studies have been focused on the flame retardancy and smoke release behavior of polyimide fibers, which are unable to provide some guidance for such materials in the field of emergency protection.

Flexible chemistry of polyimide technologies allows for structural tailoring. Therefore, performance of polyimide fibers can be modified *via* copolymerization, blending, or nanofiller reinforcement. Herein, a series of new polyimide fibers are reported based on a new design of incorporating the MDA into the highly rigid homopolyimide backbones of PMDA-PDA to synergistically solve the contradiction between the good processing ability and ultrahigh thermal stability and flame retardancy of fibers. The resultant flame-retardant polyimide fibers with a high thermal stability, intrinsic flame retardancy and low toxic smoke release can find promising applications in the field of emergency protection.

EXPERIMENTAL

Materials

Para-phenylenediamine (PDA, ≥99.5%) was purchased from Zhejiang Dragon Chemical Co., Ltd. (Hangzhou, China). Pyromellitic dianhydride (PMDA, ≥99.5%) was obtained from Rugao Leheng Chemical Co., Ltd. (Nantong, China). 4,4'-Diaminodiphenylmethane (MDA) was supplied by Wanhua Chemical Group Co., Ltd. Dimethylacetamide (DMAc) was provided by Shanghai Jinshan Jingwei Chemical Co., Ltd., and dried by 0.4 nm molecular sieve for 14 days prior to use. Nomex and Kevlar 49 fibers were manufactured by DuPont. P84 fibers were supplied by Evonik Industries, and the Suplon fiber was manufactured by Jiangsu Aoshen Hi-tech Materials Co., Ltd. (Lianyungang, China).

Fabrication of PMDA-PDA/MDA Polyimide Fibers

The poly(amic acid) (PAA) spinning dope was synthesized by mixing diamines (PDA and MDA) and equimolar amounts of PMDA in anhydrous DMAc for more than 24 h, then 15 wt% viscous spinning solution was obtained as shown in Scheme 1(a). A series of PAA spinning dopes were synthesized by verifying the PDA/MDA molar ratios (*m/n*=9/1, 8/2, 7/3, 5/5, 3/7 and 0/10).

The PAA solution was filtered and vacuum degassed for 12 h prior dry-spinning. Then, the PAA solution was transferred by a metering pump under a high pressure and was extruded through a spinneret with 144 holes into a round evaporation chamber. The solvent vaporizes immediately in the hot gas stream, increasing the polymer concentration in the filament and finally solidifying it without further drying. The solidified filaments are drawn off by rotating rolls, named as-spun PAA fibers. Afterwards, the thermal-imidization and hot-drawing process are simultaneously conducted by heating and stretching the as-spun fibers through a heating tube at a temperature of 450 °C with different drawing ratios. The obtained PAA and polyimide fibers were abbreviated as PAA-M-*x* and PI-M-*x*, respectively, where *x* means the MDA molar fraction in the diamines.

Characterizations

Micromorphologies of fibers and textiles were observed by a field-emission SEM (Hitachi SU8010). Chemical structures of as-spun PAA and PI fibers were verified *via* Fourier transform infrared spectroscopy (FTIR, Nicolet 8700) in the range of 4000–400 cm^{-1}. 2D WAXS measurements were conducted at the 16B1 beamline in Shanghai Synchrotron Radiation Facility (SSRF), and the data were analyzed using the x-Polar (Precision Works Inc., NY, USA) software package. The crystallinity (X_c) of fibers was determined by the following equation:

$$X_c = \frac{A_c}{A_c + A_a + A_m} \times 100\% \quad (1)$$

where A_c, A_a and A_m are the crystalline, amorphous and mesomorphic phase areas, respectively. The Herman's orientation factor (f_c) was calculated by the following Eq. (2):

$$f_c = [3\langle\cos^2\varphi\rangle - 1]/2 \quad (2)$$

$\langle\cos^2\varphi\rangle$ represents the orientation parameter, which can be determined by the Wilchinsky's model:

$$\langle\cos^2\varphi\rangle = \frac{\int_0^{\frac{\pi}{2}} I(\beta)\cos^2\theta\sin^2\beta\cos\beta d\beta}{\int_0^{\frac{\pi}{2}} I(\beta)\cos\beta d\beta} \quad (3)$$

where the θ is the Bragg angle, β means the azimuthal angle of crystal plane, and $I(\beta)$ is the diffraction intensity. The tensile properties of the prepared PI fibers were tested using a universal XQ-1 testing instrument with a gauge length of 20 mm at a strain rate of 1 (%)·s^{-1}. Dynamic mechanical thermal analysis (DMA) of fibers was conducted on a TA Q800 equipment under a custom mode with a pretension force of 0.1 N at a heating rate of 5 °C·min^{-1} from 50 °C to 500 °C. Thermal resistance behavior of the fibers was recorded a Netzsch 209F3 thermal gravimetric analyser at a heating rate of

https://doi.org/10.1007/s10118-022-2792-3

10 °C·min^{-1} to 900 °C in a nitrogen atmosphere.

The fabrics of Nomex, Kevlar 49, p84, Supon and PI-M-5 are made by SGA598 automatic sampling loom (Jiang Yin Tong Yuan Textile Machinery Co., Ltd., Wuxi, China). The density of warp and weft is 80 threads/10 cm, and the surface density is 120 g/m^2. Cone tests were performed under 50 kW/m^2 heat flux using a FTT cone calorimeter (Fire Testing Technology, United Kingdom) according to ISO 5660, with the dimensions of samples are 100 mm × 100 mm × 3 mm. All samples were wrapped in aluminum foil. A FTT0082 vertical burner was used to test vertical combustion performance of the fibers and textiles in accordance with ASTM D6413. The LOI values were measured on a FIRE oxygen index meter (MOTIS Combustion Technology Instrument Co., Ltd., China) according to

a Synthesis of PAA spinning dope and dry-spinning of polyimide fiber

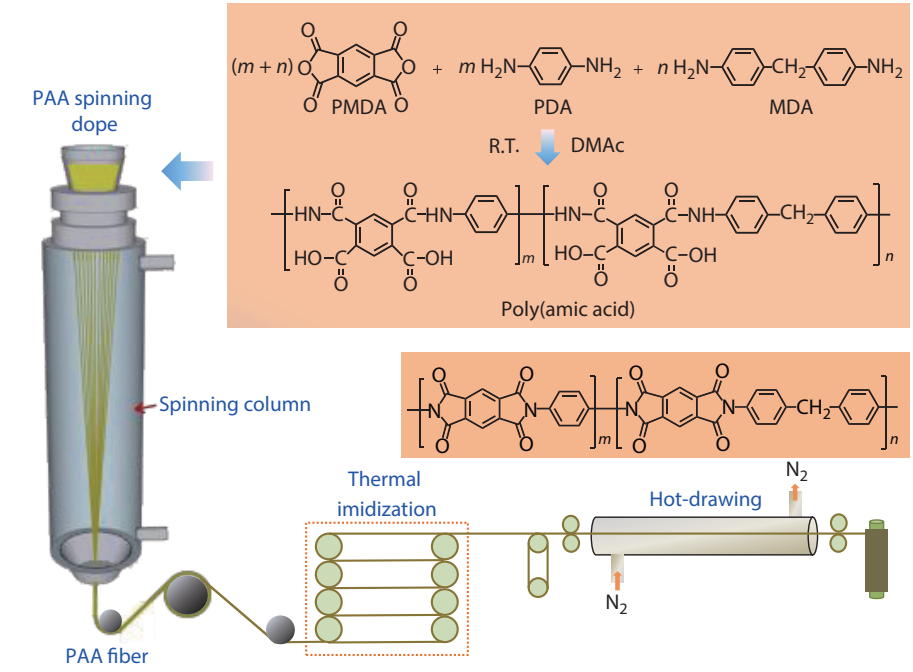

b Molecular model of PMDA-PDA, PMDA-MDA and PMDA-PDA-MDA

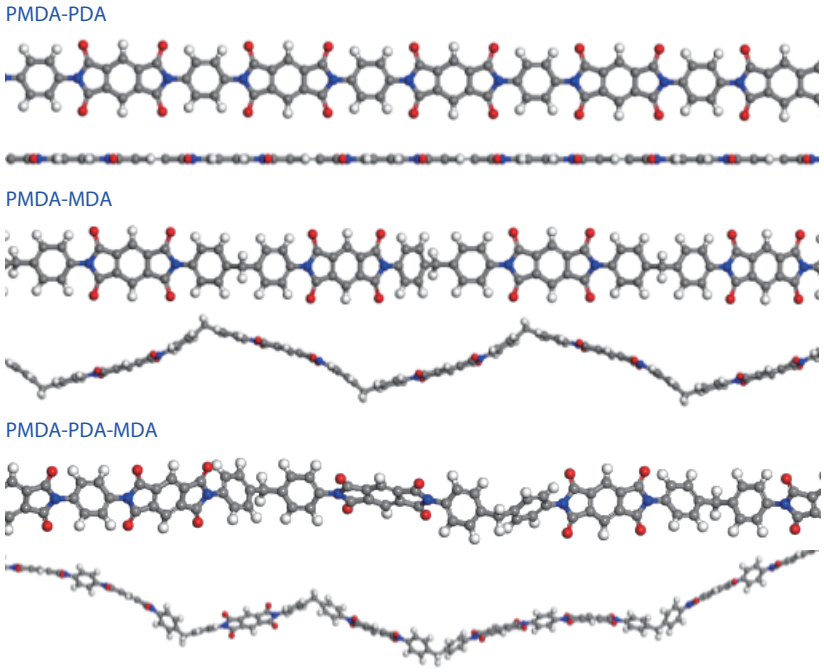

Scheme 1 (a) Synthesis of PMDA-PDA/MDA PAA spinning dope and fabrication of polyimide fibers by a dry-spinning; (b) Molecular conformation of PMDA-PDA, PMDA-MDA and PMDA-PDA/MDA.

https://doi.org/10.1007/s10118-022-2792-3

the ASTM D2863. The thermal degradation tests were carried out by TG-FTIR (PerkinElmer STA8000) under a nitrogen flow.

RESULTS AND DISCUSSION

Dry-spinning of PMDA-PDA/MDA Polyimide Fiber

Scheme 1(a) shows the schematic illustration of the dry-spinning strategy for preparing PMDA-PDA/MDA polyimide fibers, which mainly consists of synthesis of PAA spinning dope, dry-spinning PAA precursor fibers and subsequent hot-drawing. Herein, it might be expected that using the PMDA-PDA polyimide backbone would help to prepare fibers with highly thermal resistant and flame retardancy, since which demonstrates a completely coplanar conformation with a high cohesive energy density and high rigidity as derived from geometry optimization calculations using Materials Studio in Scheme 1(b). However, homo-PMDA-PDA polyimide fiber can be hardly processed continuously by the dry-spinning approach due to the following difficulty: solidified homo-PMDA-PDA PAA filaments are always brittle that cannot be drawn off by rotating rolls due to its rigid backbone structure. For this technical limitation, a new design of introducing the MDA diamine containing a flexible methylene linkage into the rigid PMDA-PDA homopolyimide backbone was proposed. Clearly, the methylene groups in MDA force the PMDA-PDA/MDA copolyimide showing a distorted and non-coplanar conformation as depicted in Scheme 1(b), which endow the PAA precursor with a good dry-spinning ability.

As a result, a series of polyimide fibers with the PDA/MDA molar ratios of 9/1, 8/2, 7/3, 5/5, 3/7 and 0/10 were successfully prepared. Fig. 1(a) shows the photographs of dry-spun polyimide fibers prepared by a large scale. Meanwhile, the fibers can be easily weaved into textiles (Figs. 1b1 and 1b2) due to their great flexibility, which is significant for their diverse practical applications. Figs. 1(c1)–1(d2) give the surface and cross-section morphologies of the PI-M-5 fiber, which shows a smooth surface and a dense inner structure. Moreover, the dry-spun PI-M-5 fiber exhibits a characteristic dumbbell or dog bone shape, which is mainly affected by the solvent diffusion and evaporation behavior in the dry-spinning. As the solvent evaporates from the spinning dope, the outer part of the filament solidifies before the inner part, which causes radial inhomogeneity within each filament. The outer part collapses inwards to produce the dog bone shape.[24] Therefore, key parameters associated with the fiber's micromorphology always consist of the concentration of polymer solution, the interaction between polymer and solvent, the spinning temperature, *etc*. Comparatively, the PI-M-10 fiber, namely, homo-PMDA-MDA polyimide, shows a circular cross-section with an inner structure, further indicating that the introduction of MDA can improve the spinnability of the homo-PMDA-PDA.

The chemical structures of as-spun PAA and hot-drawn polyimide fibers were characterized by FTIR. It is noticeable from the Fig. 2(a) that the as-spun PAA fibers with different PDA/MDA molar ratios are characterized by the following bands: a mode near 1667 cm^{-1} assigned to the hydrogen-bonded carboxylic acid pairs, a characteristic aromatic ring stretching mode near 1597 cm^{-1}, both of which are attributed to the amide bonds. Additionally, the presence of characteristic absorption for carbonyl group of the imide ring at 1773 and 1715 cm^{-1}, and a characteristic band for C—N vibration at 1357 confirms the formation of imide rings during the fiber spinning.[25] Thus, an advantage for preparing polyimide fibers *via* the dry-spinning is that partial amic acid moieties will be thermally imidized to imide in the high-temperature evaporation chamber, namely, the solidification and partial imidization taking place simultaneously, which is beneficial for improving the stability and tensile strength of as-spun PAA fibers. After hot-drawing, the spectroscopic characteristics of PAA precursors at 1667 and 1597 cm^{-1} were absent and the absorption band at 1703 cm^{-1} representing the C=O

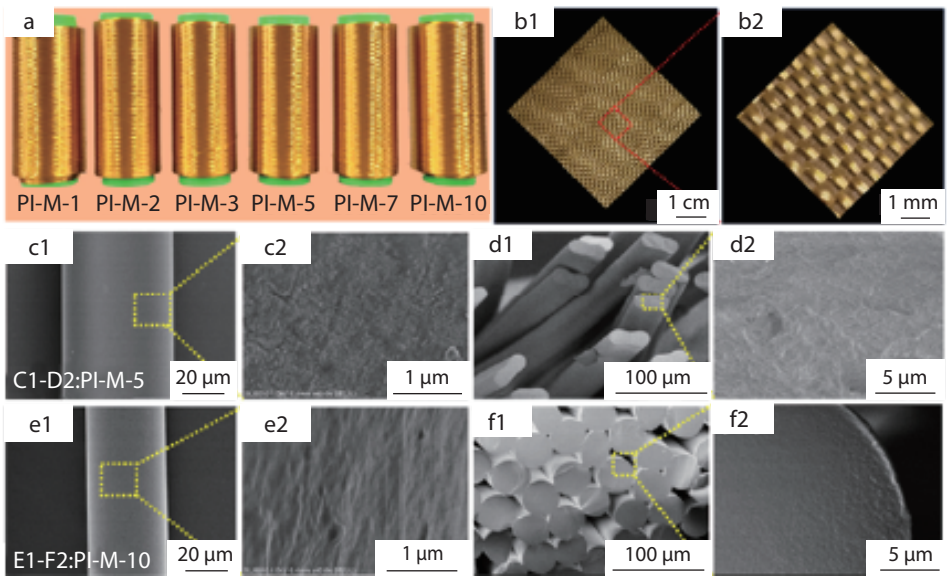

Fig. 1 (a) Photographs of dry-spun polyimide fibers; (b1, b2) Digital photos of the polyimide fiber woven into textile with different magnifications; (c1–d2) Surface and cross-section morphologies of PI-M-5 fiber; (e1–f2) Surface and cross-section morphologies of PI-M-10 fiber.

https://doi.org/10.1007/s10118-022-2792-3

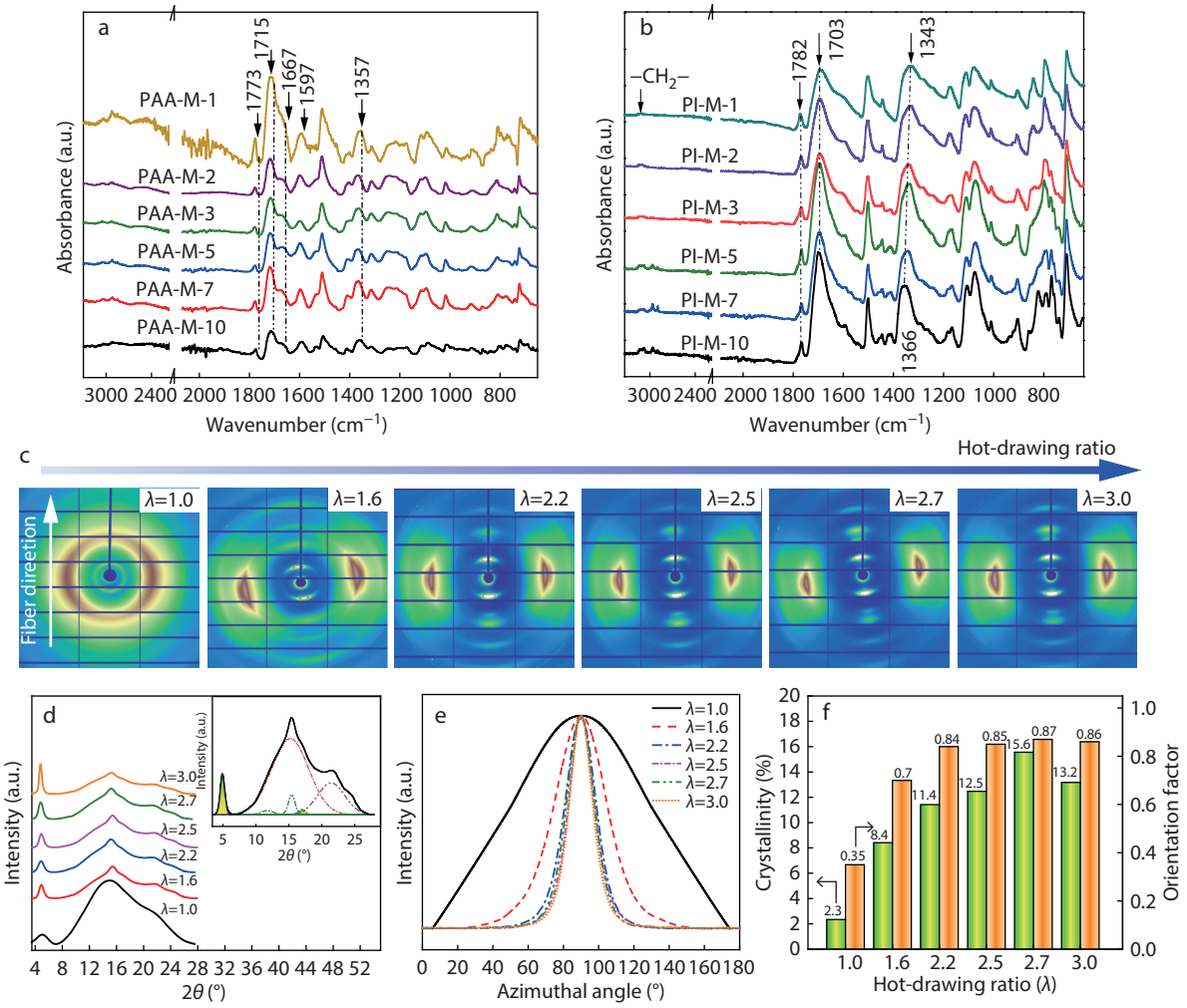

Fig. 2 (a, b) FTIR spectra of as-spun PAA and hot-drawn PI fibers with different PDA/MDA molar ratios; (c) Two-dimensional WAXS patterns of the PI-M-5 fiber thermally stretched with different draw ratios at 450 °C; (d) 1D integrated WAXS intensities for the PI-M-5 fiber; (e) Azimuthal profiles of the scattering peak at 2θ=5° with hot-drawing ratios for the PI-M-5 fiber; (f) Degrees of orientation factor and crystallinity for different hot-drawn PI-M-5 fibers.

symmetrical stretching in imide rings became stronger, indicating the full imidization of as-spun fibers.

In principle, a hot-drawing post-treatment plays a crucial role in the formation of high orientation of rigid-rod polyimide chains crystallization of fibers, and always results in an improved mechanical strength. In Fig. 2(c), 2D WAXS patterns of the PI-M-7 fiber containing 30 mol% of PDA with different hot-drawing ratios (λ) are presented. The unstretched fiber (λ=1) exhibits obscure equatorial arcs, named "amorphous halos", indicating a relatively low ordering degree of the lateral stack of polymer chains. Dramatic changes in the 2D WAXS patterns occur as increasing the drawing ratio. The equatorial and meridianal intensities become intense, revealing the formation of semi-crystalline structure in fibers and orientation of polymer chains. Correspondingly, the 1D integrated intensity profile obtained from Fig. 2(c) is presented in Fig. 2(d). Regardless of the drawing ratio, all drawn fibers exhibit three Bragg scattering streaks at 2θ=4.8°, 15.1° and 21.9°, which corresponds to *d*-spacings of 14.7, 4.7 and 3.26 Å, respectively. Moreover, an increase in the scattering intensity at 2θ=4.8° with respect to the drawing-ratio is observed, further implying the strain-induced crystallization and oriented crystalline structure subsequently forms in the hot-drawing process. Curve-fitting deconvolution of the 1D WAXS profiles performed using Peak-fit software suggests the coexistence of crystalline, mesomorphic and amorphous regions in drawn PI-M-5 fibers. As shown in Fig. 2(e), the polymer chain orientation, as evaluated by full width at half-maximum (FWHM) of the azimuthal intensity distribution of the scattering intensity at 2θ=4.8°, increases significantly after hot-drawing revealed by the decreased FWHM. Detailed crystallinity and Herman's orientation factor with drawing ration are plotted in Fig. 2(f), both of which tend to be larger with the drawing ratio λ. The PI-M-5 fiber with λ=2.7 shows the highest crystallinity of 15.6% and orientation factor of 0.87. Further raising the λ to 3.0 results in slight decreases in crystallinity and orientation factor.

Mechanical Property, Thermal Stability and Flame-resistance of the Resultant Fiber

As manifested in Fig. 3(a), the unstretched PI-M-5 fiber has an

https://doi.org/10.1007/s10118-022-2792-3

initial tensile strength and modulus of 1.17 and 12.13 cN/dtex, and reaches 65% elongation before failure. An improvement of mechanical property of the fiber after hot-drawing can be obtained.[26,27] At λ=2.7, the fiber shows an optimum breaking strength and modulus (5.15 and 71.83 cN/dtex, respectively), 340% and 492% higher than those of the unstretched fiber. Fig. 3(b) compares the resultant polyimide fibers with different PDA/MDA molar ratios. It is obvious that the PI-M-5 fiber with 50 mol% of MDA shows the highest tensile strength of 5.3 cN/dtex with a modulus of 83.0 cN/dtex. Attributed to the high rigidity of PDA, the PI-M-3 containing 70 mol% PDA exhibits the highest modulus of 97.0 cN/dtex with moderate strength of 2.3 cN/dtex.

The tanδ curves of resultant polyimide fibers with different PDA/MDA molar ratios as a function a temperature are presented in Fig. 3(c), where the relaxation peaks can be regarded as the T_g. T_gs of PI-M-5, 7 and 10 are 421 °C, 418 and 389, respectively, indicating that more PDA contents in backbone are beneficial for improving the T_g of polyimide fibers. Unfortunately, no obvious relaxation peaks can be detected as the molar content of PDA over 70 mol%, which may be mainly attributed to the relatively higher rigidity of polyimide backbones and limited segmental motion as further increasing the PDA content. The representative TGA and derivative thermogravimetric (DTG) diagrams of polyimide fibers are

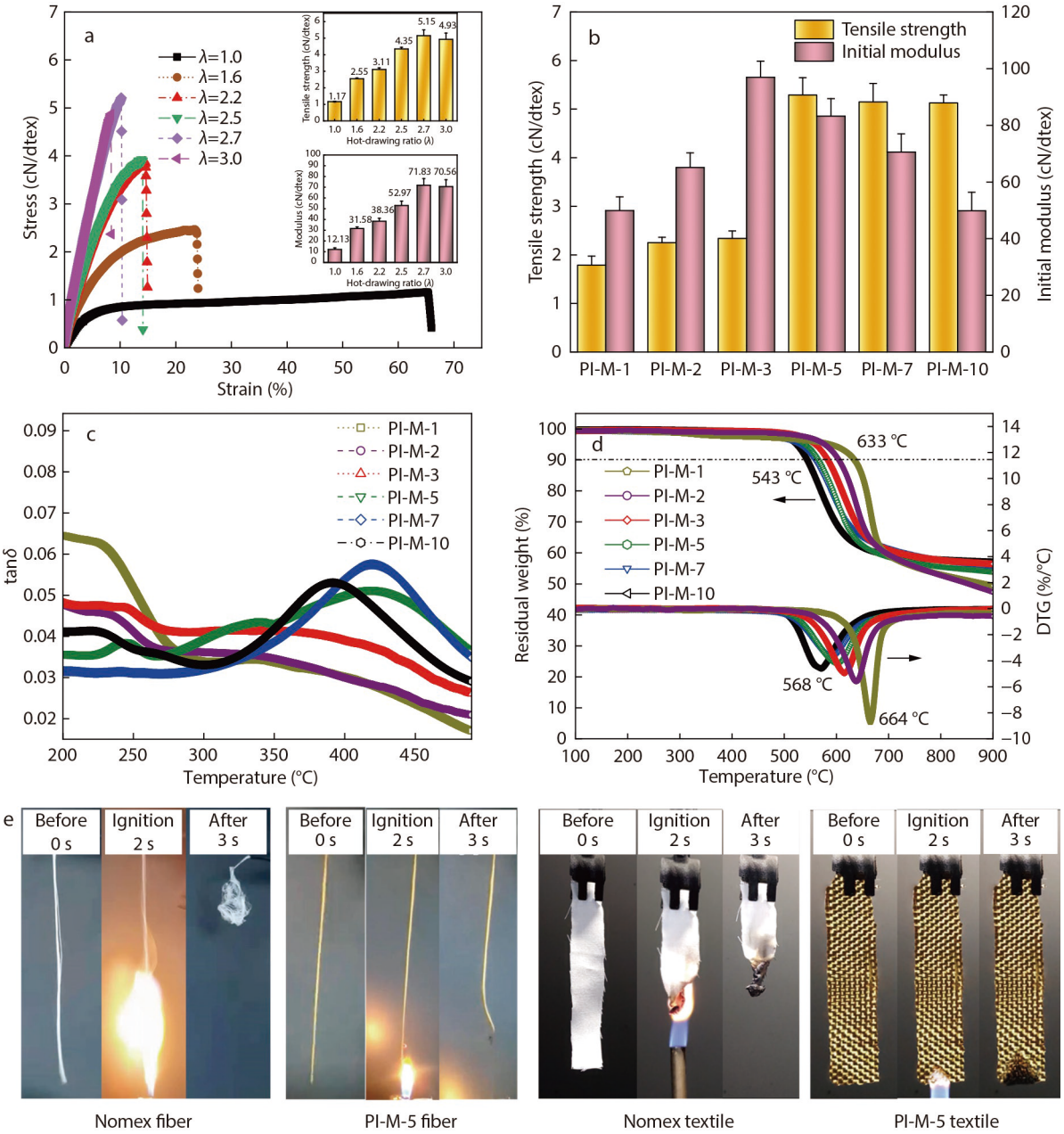

Fig. 3 (a) Stress-strain curves and detail tensile properties of the PI-M-5 fiber with different drawn ratios; (b) Mechanical tensile properties of the polyimide fibers with different PDA/MDA molar ratios; (c, d) DMA and TGA curves of polyimide fibers containing different MDA contents; (e) Ignition tests of the commercial Nomex fiber and PI-M-5 fiber and their textiles.

https://doi.org/10.1007/s10118-022-2792-3

shown in Fig. 3(d). As observed from TGA curves, the temperature of corresponding to 10 wt% ($T_{10\%}$) weight loss of PI-M-10 is 543 °C in nitrogen, while the $T_{10\%}$ of the PI-M-1 increases to 633 °C. In addition, the temperature corresponding to maximum mass loss rate (T_{max}) of PI-M-10 is approximately 96 °C lower than that of the PI-M-1, further indicating that a higher PDA content tends to endow the fiber with a better thermal resistance.

As a good candidate for the special thermal protection material, the flame resistance is also pivotal. Nomex fabric is widely used in thermal protection and aerospace fields due to its excellent heat resistance. PI-M-5 fiber and fabric were used as the typical example to compare with Nomex fiber and fabric in terms of flame retardancy. Fig. 3(e) presents the vertical burning tests of the Nomex fiber, PI-M-5 fiber and their textiles at 0, 2 and 3 s. The Nomex fiber and its textile can be easily ignited. Comparatively, the PI-M-5 fiber and textile are hard to ignite and show a rapid self-extinguishing property after removal of fire, indicating their superb flame resistance. The LOI test is always used to rank the relative flammability of polymer and the rating can be served as an indication of polymer's acceptability for applications.[28] As listed in Table 1, the PI-M-5 shows a relatively high limited oxygen index (LOI) value of 39% and UL-94 ASTM D6413 V-0 rating, further illustrating a better flame resistance than other commercial fire-retardant polymeric fibers, including the Suplon polyimide fiber (LOI=36), P84 polyimide fiber (LOI=38), Nomex fiber (LOI=29) and the Kevlar 49 fiber (LOI=31), whose chemical structures and mechanical properties are shown in Figs. S1 and S2 in the electronic supplementary information (ESI).

Heat and Smoke Release During the Thermal Degradation

For further exploring the flame retardancy of prepared polyimide fibers, the cone calorimeter tests are carried out, which always can truly simulate the combustion of polymers in a real fire situation.[29] The heat release rate (HRR) curves of PI-M-5 and the referenced Suplon, P84, Nomex and Kevlar 49 fibers are shown in Fig. 4(a) and Table 1. Remarkably, the PI-M-5 fiber exhibits the minimum HRR value (14.1 kW/m^2) in the longest ignition time of 813 s during combustion, indicating the PI-M-5 fiber owning the lowest flammability with low full-scale hazards. The long time to ignition is beneficial for preventing flame spread and suppress the production of toxic smoke. Relatively, both the Nomex and Kevlar 49 fibers release a large amount of heat in a short time. For example, the Nomex fiber ignites after 23 s and rapidly reaches a HRR value of 140.6 kW/m^2, 900% higher than that of the PI-M-5, finally burning out at 220 s. Even compared with the commercial Suplon and P84 polyimide fibers as well as the other reported flame retardant polymeric fibers as shown in Table 1, the PI-M-5 shows a higher inflammable degree. Since that total heat release (THR) is the integrated value of HRR as a function of ignition time, the THR of these fibers presents a similar tendency of variation with HRR as shown in Fig. 4(b). The THR values of P84 and Nomex fibers are 8.60 and 7.87 MJ/m^2, respectively, whereas the THR of PI-M-5 is only 4.49 MJ/m^2. The lower HRR and THR values of the PI-M-5 fiber reflect its better flame retardancy. Moreover, the damaged char lengths for different fibers in the vertical burning test are shown in the Table S1 (in ESI). Clearly, the PI-M-5 shows the lowest damaged char length of 5 mm, which is only one-tenth and quarter of the Nomex and Kevlar 49 fabrics, further indicating its better flame retardancy, which can be explained based on the morphology of the residual char and the evolved gases from pyrolysis.

From the digital images of the residual char after cone calorimeter test (Fig. S3 in ESI), the *para*-aramid Kevlar 49 fabric almost burns entirely out and generates merely no char layers besides some carbonaceous particles, indicating its poor char-forming ability. For the *meta*-aramid Nomex fabric, a substance similar to a molten layer tightly adheres to the surface of aluminium foil after the cone calorimetry test. Comparatively speaking, the three polyimide fabrics (especially for the PI-M-5) present the same aspect as the beginning of the measurement expect for the black colour while these residues are crumbly and have no mechanical properties, indicating the higher char-forming ability of polyimide fibers in relative to the aramid fibers due to the abundant phenyl and imide rings. The TGA curves can further demonstrate this point of view from the relatively higher char residues of the PI-M-5 (58.5%) than the Kevlar 49 (43.2%) and Nomex (44.9%) (Figure S4). It could be concluded that the inherent backbone rigidity and high cohesive energy density of the designed

Table 1 Combustion results of typical thermal-resistance polymeric fibers.

Samples	LOI (%)	TTI (s)	HRR (kW/m^2)	THR (MJ/m^2)	SPR (m^2/s)	TSP (m^2/m^2)	Ref.
PI-M-5	39	813	14.1	4.49	0.0015	0.065	This work
Suplon	36	614	40.2	4.92	0.0035	0.036	This work
P84	38	600	41.6	8.60	0.0021	0.285	This work
Nomex	31	220	140.6	7.87	0.025	0.534	This work
Kevlar 49	31	220	94.4	5.23	0.020	0.323	This work
PA/alginate(50/50)	–	26	175.6	10.9	–	1.1	[30]
PA6	23	90	1192	98.9	–	–	[31]
PA6-D10	31.1	85	952	84.9	–	–	[31]
Polyester	–	83	335.8	13.5	–	–	[32]
Alginate	48	82	36.9	2.5	–	–	[32]
FRV/PMIA(50/50)	–	45	73.5	5.0	–	–	[19]
PAN	17.8	1.7	537.5	17.2	0.103	–	[33]
2 wt% TA-MoS_2/PA	26	2.9	332.8	12.1	0.068	–	[33]
40% APP/PP	–	19.3	254.8	54.4	0.013	–	[34]
Cotton/alginate(50/50)	–	40	66	7.0	0.004	–	[20]
2 wt% MPZSN-MoS_2/PAN	–	-	86.2	15.6	–	–	[35]

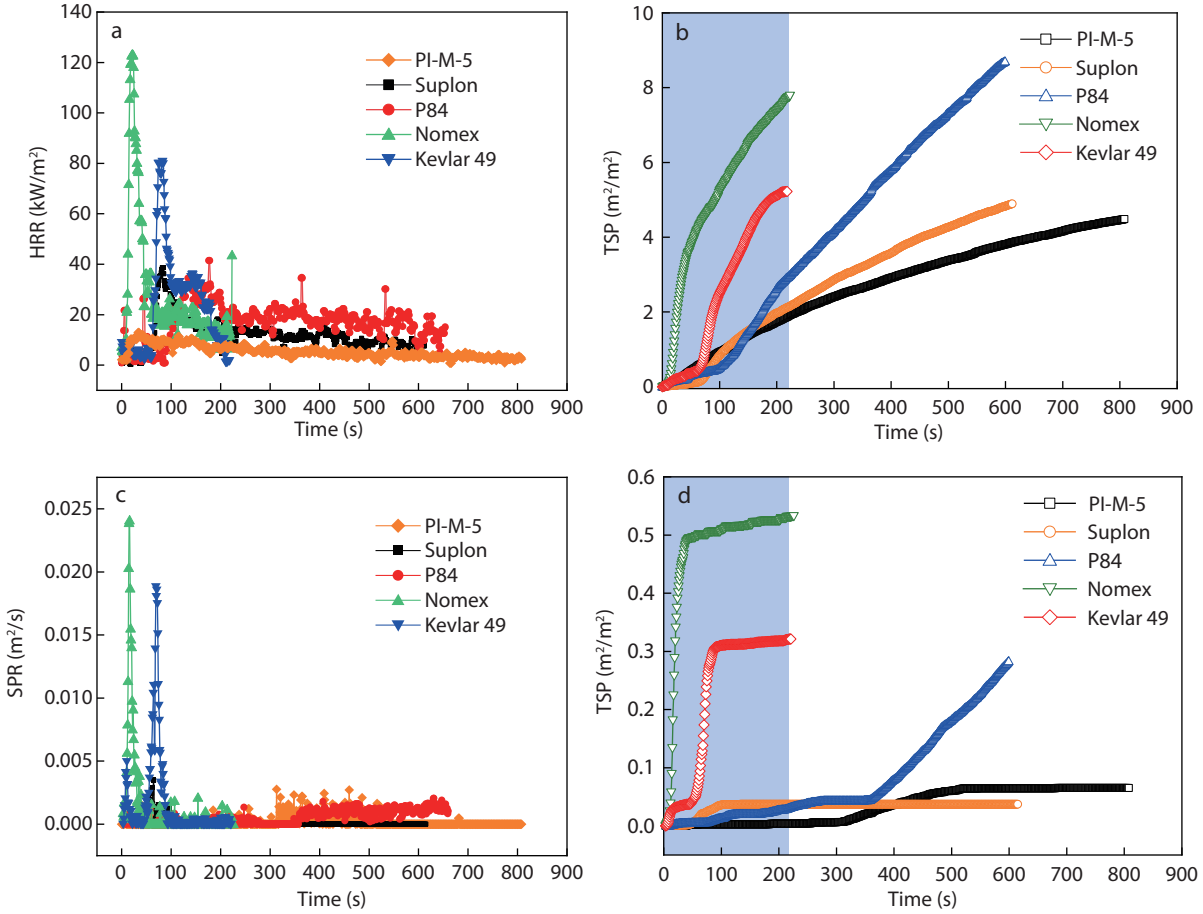

Fig. 4 (a) HRR, (b) THR, (c) SPR and (d) TSP curves of PI-M-5 and the commercial Suplon polyimide, P84 polyimide, Nomex and Kevlar 49 fibers obtained from cone calorimeter.

polyimide with abundant benzene and imide rings endow the fiber with a high thermal stability and char forming ability as well as an excellent flame retardancy.

As for the evolved gases, the volatile emission during burning, such as steam, CO_2, toxic CO and HCN, *etc*, is regarded as another kind of factor affecting the combustion behavior of materials. As seen in Figs. 4(c) and 4(d) and Table 1, the peak smoke production rate (SPR) and total smoke production (TSP) of PI-M-2 are 0.0015 m^2/s and 0.065 m^2/m^2, respectively, which are strongly lower than those of the Nomex (SPR=0.025 m^2/s, TSP=0.534 m^2/m^2) and Kevlar 49 (SPR=0.020 m^2/s, TSP=0.323 m^2/m^2) fibers. Therefore, the considerable reductions of volatile emission indicate effective decrease in the fire hazard of the PI-M-5 fiber. For the combustible CO gas as shown in Fig. S5 (in ESI), the peak CO production of PI-M-5, Suplon, P84, Nomex and Kevlar 49 fabrics is 0.0007, 0.0035, 0.0034, 0.0022 and 0.0017 g/s, respectively. Obviously, the peak CO production of PI-M-5 is at the rock bottom level, only one-third of the Nomex fabric. This considerable reduction in combustible CO release also benefits the improvement of flame retardancy and the decrease in the fire hazard, which can potentially reduce the death rate in a real fire. Accordingly, the synergistic mechanism of flame retardancy in prepared PI-M-5 fiber is attributed to the combined contribution in the char forming ability and reduced release of combustible gas.

For getting more useful information of the pyrolysis gaseous products during burning, the thermal degradation of Nomex and PI-M-5 fibers were investigated by the TG-FTIR technique. 3D TG-FTIR spectra and the corresponding absorption peaks of evolved pyrolysis products at different temperatures obtained from the thermal decomposition of the Nomex and PI-M-5 fibers are shown in Figs. 5(a) and 5(b), respectively. There is almost no thermal decomposition for the Nomex fiber below 400 °C as no absorption peaks can be detected in the FTIR. With increasing temperature from 500 °C to 650 °C, absorption bands at 2375–2290 and 1763 cm^{-1} assigned to CO_2, and 1618 and 1500 cm^{-1} corresponding to the combustible benzene and benzene derivatives, can be detected, and their absorption intensity increases continuously.[36] A comparison of the TG-FTIR spectra shows that the species of the gaseous products obtained from PI-M-5 is similar with the Nomex fiber, but with variations of decomposition temperatures. As shown in Fig. 5(b), PI-M-5 starts to emit gases at a higher temperature of 600 °C with a lower gas content, which also contributes to its high flame retardancy.

The micromorphology of char residues collected after cone tests of Nomex and PI-M-2 textiles are analyzed by SEM as

https://doi.org/10.1007/s10118-022-2792-3

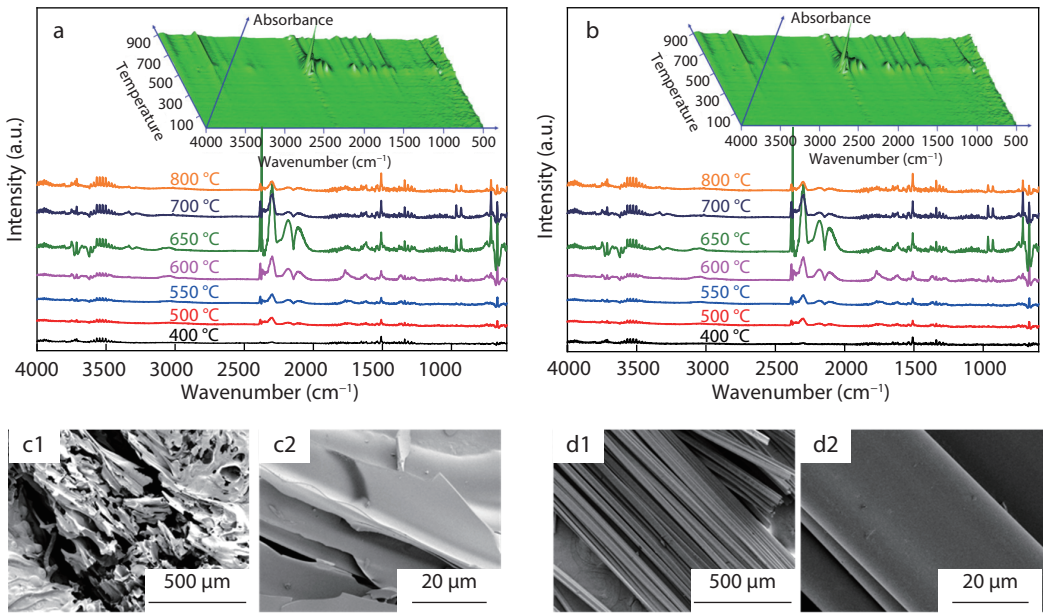

Fig. 5 Three-dimensional TG-FTIR spectra of gasified pyrolysis products for (a) Nomex and (b) PI-M-5 fiber, and SEM images of the char residues of (c1, c2) Nomex and (d1, d2) PI-M-5 fiber.

shown in Figs. 5(c1)–5(d2). Apparently, the char formed by Nomex is dispersed and discontinuous with numerous crevices and opening voids, which is mainly resulted from the breakage of its backbone and release of the volatiles. As for the PI-M-5, the fibrous morphology can be totally preserved and a complete and continuous char layer is formed, which is significant for the inhibition of heat and combustible volatiles transfer and results in an enhanced flame retardancy in condensed phase.

CONCLUSIONS

In summary, a series of high-performance polyimide fibers based on the PDA, MDA and PMDA were successfully fabricated by a scale dry-spinning method, where the solidification of filaments and partial imidization of the PAA precursors take place simultaneously. The resultant polyimide fiber containing 50 mol% of PDA respectively shows an optimum mechanical property with the tensile strength of 5.3 cN/dtex and a modulus of 83.0 cN/dtex. As raising the PDA content to 90 mol% in diamines, the $T_{10\%}$ of the fiber increases to 633 °C, approximately 90 °C higher than that of the homo-PMDA-MDA fiber, showing an excellent thermal stability. Moreover, the prepared fiber presents a superb flame retardancy with the LOI of 39% and a rapid self-extinguishing property. The cone calorimeter results demonstrate that the heat release rate and smoke production rate for the polyimide fiber are extraordinarily low, which are almost 10% and 6% of the commercial Nomex fiber. Moreover, the char residues' micromorphology of the polyimide fiber presents a complete and continuous char layer reserved after combustion. Therefore, it can be concluded that the polyimide fibers can be served as a better thermal protective material than those commercial inherent flame retardant fibers, such as Nomex, Kevlar 49 and P84 fibers, as well as those of modified flame retardant fibers, making them very suitable for manufacturing fireproof fabrics for firefighters, mine workers, soldiers, *etc.*

NOTES

The authors declare no competing financial interest.

Electronic Supplementary Information

Electronic supplementary information (ESI) is available free of charge in the online version of this article at http://doi.org/10.1007/s10118-022-2792-3.

ACKNOWLEDGMENTS

This work was financially supported by the National Natural Science Foundation of China (Nos. 51903038 and 21975040), the Scientific Research Innovation Plan of Shanghai Education Commission (No. 2019-01-07-00-03-E00001), the Natural Science Foundation of Shanghai (No. 21ZR1400200) and the Project "Fiber materials and products for emergency support and public safety" from Jiangsu New Vision Advanced Functional Fiber Innovation Center Co., Ltd. (No. 2021-fx020204).

REFERENCES

1 He, W. T.; Song, P. A; Yu, B.; Fang, Z. P.; Wang, H. Flame retardant polymeric nanocomposites through the combination of nanomaterials and conventional flame retardants. *Prog. Mater. Sci.* **2020**, *114*, 100687.
2 Liu W.; Zhang, S.; Chen, X. S.; Yu, L. H.; Zhu, X. J.; Feng, Q. L. Thermal behavior and fire performance of nylon-6,6 fabric modified with acrylamide by photografting. *Polym. Degrad. Stabil.* **2010**, *95*, 1842–1848.
3 Yu, S. R.; Xia, Z. Y.; Kiratitanavit, W.; Thota, S.; Kumar, J.; Mosurkal,

R.; Nagarajan, R. Unusual role of labile phenolics in imparting flame resistance to polyamide. *Polym. Degrad. Stabil.* **2020**, *175*, 109103.
4 Jiang, P.; Zhao, Q.; Zhang, S.; Gu, X. Y.; Hu, Z. W.; Xu, G. Z. Flammability and char formation of polyamide 66 fabric: chemical grafting versus pad-dry process. *Ind. Eng. Chem. Res.* **2015**, *54*, 6085–6092.
5 Kim, I.; Thompson, A. L.; Kim, S. C.; Hamins, A.; Bundy, M.; Nazaré, S.; Davis, R.D.; Zammarano, M. Demonstration of an all-in-one solution for fire safe upholstery furniture: a benign backcoating for smoldering and flame-resistant cover fabrics. *Fire Mater.* **2022**, *46*, 677–693.
6 Li, Y.; Li, X.; Pan, Y. T.; Xu, X.; Song, Y.; Yang, R. Mitigation the release of toxic PH3 and the fire hazard of PA6/AHP composite by MOFs. *J. Hazard. Mater.* **2020**, *395*, 122604.
7 Norouzi, M.; Zare, Y.; Kiany, P. Nanoparticles as effective flame retardants for natural and synthetic textile polymers: application, mechanism, and optimization. *Polym. Rev.* **2015**, *55*, 531–560.
8 Wang, X.; Kalali, E. N.; Wan, J. T.; Wang, D. Y. Carbon-family materials for flame retardant polymeric materials. *Polym. Sci.* **2017**, *69*, 22–46.
9 Meng, D.; Guo, J.; Wang, A. J.; Gu, X. Y.; Wang, Z. W.; Jiang, S. L.; Zhang, S. The fire performance of polyamide 66 fabric coated with soybean protein isolation. *Prog. Org. Coat.* **2020**, *148*, 105835.
10 Zhou, Q.; Wu, W.; Zhou, S.; Xing, T.; Sun, G.; Chen, G. Polydopamine-induced growth of mineralized γ-FeOOH nanorods for construction of silk fabric with excellent superhydrophobicity, flame retardancy and UV resistance. *Chem. Eng. J.* **2020**, *382*, 122988.
11 Breuer, R.; Zhang, Y. X.; Erdmann, R.; Hernandez, O. E. V. Development and processing of flame retardant cellulose acetate compounds for foaming applications. *J. Mater. Sci.* **2020**, *137*, 48863.
12 Li, P.; Wang, B.; Xu, Y. J.; Jiang, Z.; Dong, C.; Liu, Y.; Zhu, P. Ecofriendly flame-retardant cotton fabrics: preparation, flame retardancy, thermal degradation properties, and mechanism. *ACS Sustainable Chem. Eng.* **2019**, *7*, 19246–19256.
13 Zhang, Y.; Tian, W.; Liu, L.; Cheng, W.; Wang, W.; Liew, K. M.; Wang, B.; Hu, Y. Eco-friendly flame retardant and electromagnetic interference shielding cotton fabrics with multi-layered coatings. *Chem. Eng. J.* **2019**, *372*, 1077–1090.
14 Liu, Y.; Pan, Y. T.; Wang, X.; Acuña, P.; Zhu, P.; Wagenknecht, U.; Heinrich, G.; Zhang, X. Q.; Wang, R.; Wang, D.Y. Effect of phosphorus-containing inorganic–organic hybrid coating on the flammability of cotton fabrics: Synthesis, characterization and flammability. *Chem. Eng. J.* **2016**, *294*, 167–175.
15 Maddalena, L.; Carosio, F.; Gomez, J.; Saracco, G.; Fine, A. Layer-by-layer assembly of efficient flame retardant coatings based on high aspect ratio graphene oxide and chitosan capable of preventing ignition of PU foam. *Polym. Degrad. Stabil.* **2019**, *152*, 1–9.
16 Qiu, X.; Li, Z.; Li, X.; Zhang, Z. Flame retardant coatings prepared using layer by layer assembly. *Chem. Eng. J.* **2018**, *334*, 108–122.
17 Zhang, X.; Shi, M. Flame retardant vinylon/poly (m-phenylene isophthalamide) blended fibers with synergistic flame retardancy for advanced fireproof textiles. *J. Hazard. Mater.* **2019**, *365*, 9–15.
18 Wang, B.; Li, P.; Xu, Y. J.; Jiang, Z. M.; Dong, C. H.; Liu, Y.; Zhu, P. Bio-based, nontoxic and flame-retardant cotton/alginate blended fibres as filling materials: thermal degradation properties, flammability and flame-retardant mechanism. *Compos. Part B: Eng.* **2020**, *194*, 108038.
19 Carosio, F.; Blasio, A. D.; Cuttica, F.; Alongi, J.; Malucelli, G. Flame retardancy of polyester and polyester-cotton blends treated with caseins. *Ind. Eng. Chem. Res.* **2014**, *53*, 3917–3923.
20 Zhang, Q. H.; Dong, J.; Wu, D. Z.; Yang, S. Y. in *Advanced Polyimide Fibers*. Elsevier, Inc., Oxford, **2018**, p. 67–92.
21 Bhat, G.; Schwanke, R. Thermal properties of a polyimide fiber. *J. Therm. Anal. Calorim.* **1997**, *49*, 399–405.
22 Imura, Y.; Hogan, R.; Jaffe, M. in *Advances in Filament Yarn Spinning of Textiles and Polymers*. Elsevier, Oxford, **2014**, p. 187–202.
23 Snyder, R. W.; Thomson, B.; Bartges, B. Czerniawski, D.; Painter, P. C. FTIR studies of polyimides: thermal curing. *Macromolecules* **1989**, *22*, 4166–4172.
24 Bao, F.; Zhang, R.; Dong, Z. X.; Qi, F. L.; Cai, Y. C.; Dai, X. M.; Ji, X. L.; Qiu, X. P. Comparison of high-performance polyimide copolymer fibers containing pyrimidine moieties based on coplanar structures. *Polymer* **2021**, *231*, 124113.
25 He, W. J.; Kong, C.; Cai, Y. D.; Ye, L.; Chen, S.T.; Li, S. H.; Zhao, X. W. Thermal stability enhancement of oriented polyethylene by formation of epitaxial shish-kebab crystalline structure. *Polym. Degrad. Stabil.* **2022**, *195*, 109771.
26 Wang, Q. Z.; Liu, C.; Xu, Y. J.; Liu, Y.; Zhu, P.; Wang, Y. Z. Highly efficient flame retardation of polyester fabrics *via* novel DOPO-modified sol-gel coatings. *Polymer* **2021**, *226*, 123761.
27 Sonnier, R.; Viretto, A.; Dumazert, L.; Gallard, B. A method to study the two-step decomposition of binary blends in cone calorimeter. *Combust. Flame* **2016**, *169*, 1–10.
28 Gu, W. W.; Dong, Z. F.; Zhang, A. Y.; Ma, T. Y.; Hu, Q.; Wei, J. F.; Wang, R. Functionalization of PET with carbon dots as copolymerizable flame retardants for the excellent smoke suppressants and mechanical properties. *Polym. Degrad. Stabil.* **2022**, *195*, 109766.
29 Ding, Y.; Stoliarov, S. I.; Kraemer, R. H. Pyrolysis model development for a polymeric material containing multiple flame retardants: relationship between heat release rate and material composition. *Combust. Flame* **2019**, *202*, 43–57.
30 Zhang, F. Q.; Wang, B.; Xu, Y. J.; Li, P.; Liu, Y.; Zhu, P. Convenient blending of alginate fibers with polyamide fibers for flame-retardant non-woven fabrics. *Cellulose* **2020**, *27*, 8341–8349.
31 Zhang, S.; Fan, X.; Xu, C.; Ji, P.; Wang, C.; Wang, H. An inherently flame-retardant polyamide 6 containing a phosphorus group prepared by transesterification polymerization. *Polymer* **2020**, *207*, 122890.
32 Li, P.; Wang, Q. Z.; Wang, B.; Liu, Y. Y.; Xu, Y. J.; Liu, Y.; Zhu, P. Blending alginate fibers with polyester fibers for flame-retardant filling materials: Thermal decomposition behaviors and fire performance. *Polym. Degrad. Stabil.* **2021**, *183*, 109470.
33 Peng, H.; Wang, D.; Fu, S. Tannic acid-assisted green exfoliation and functionalization of MoS_2 nanosheets: Significantly improve the mechanical and flame-retardant properties of polyacrylonitrile composite fibers. *Chem. Eng. J.* **2020**, *384*, 123288.
34 Jung, D.; Bhattacharyya, D. Keratinous fiber based intumescent flame retardant with controllable functional compound loading. *ACS Sustainable Chem. Eng.* **2018**, *6*, 13177–13184.
35 Peng, H.; Wang, D.; Li, M.; Zhang, L.; Liu, M.; Fu, S. NP-Zn-containing 2D supermolecular networks grown on MoS_2 nanosheets for mechanical and flame-retardant reinforcements of polyacrylonitrile fiber. *Chem. Eng. J.* **2019**, *372*, 873–885.
36 Zhu, H. Q.; Zhao, H. R.; Wei, H. Y.; Wang, W.; Wang, H. R.; Li, K.; Lu, X. X.; Tan, B. Investigation into the thermal behavior and FTIR micro-characteristics of re-oxidation coal. *Combust. Flame* **2020**, *216*, 354–368.

https://doi.org/10.1007/s10118-022-2792-3